Title

Structure and energy transfer pathways of the plant photosystem I-LHCI supercomplex

Michihiro Suga[1], Xiaochun Qin[1,2], Tingyun Kuang[2] and Jian-Ren Shen[1,2]

[1]Research Institute for Interdisciplinary Science, Graduate School of Natural Science and Technology, Okayama University, Tsushima Naka 3-1-1, Okayama 700-8530, Japan.

[2]Photosynthesis Research Center, Key Laboratory of Photobiology, Institute of Botany, Chinese Academy of Sciences, Beijing 100093, China.

Corresponding authors: Tingyun Kuang (kuangty@ibcas.ac.cn) and Jian-Ren Shen (shen@okayama-u.ac.jp)

Short Title: Structure of plant PSI-LHCI supercomplex

Abstract

Photosystem I (PSI) is one of the two photosystems in oxygenic photosynthesis, and absorbs light energy to generate reducing power for the reduction of $NADP^+$ to NADPH with a quantum efficiency close to 100%. The plant PSI core forms a supercomplex with light-harvesting complex I (LHCI) with a total molecular weight of over 600 kDa. Recent X-ray structure analysis of the PSI-LHCI membrane-protein supercomplex has revealed detailed arrangement of the light-harvesting pigments and other cofactors especially within LHCI. Here we introduce the overall structure of the PSI-LHCI supercomplex, and then focus on the excited energy transfer (EET) pathways from LHCI to the PSI core and photoprotection mechanisms based on the structure obtained.

Introduction

Oxygenic photosynthesis is catalyzed by two photosystems, photosystem II (PSII) and photosystem I (PSI). Both photosystems capture light energy from the sun; PSII oxidizes water molecules to generate electrons, protons and molecular oxygen, whereas PSI accepts electrons from PSII and transfers them to ferredoxin, thereby generating the reducing power for reduction of $NADP^+$ into NADPH. The core complex of PSI is

largely conserved from prokaryotic cyanobacteria to eukaryotic higher plants. Cyanobacterial PSI core contains 12 subunits and forms a trimer with a total molecular weight of 1,068 kDa. On the other hand, higher plant PSI exists in a monomeric form, and is surrounded by four transmembrane light-harvesting complex I (LHCI) subunits Lhca1-Lhca4 to form a PSI-LHCI supercomplex, which has a total molecular weight over 600 kDa. The function of LHCI is to harvest light energy and transfer them to the PSI core to initiate the charge separation and electron transfer reactions. One of the most significant features of the plant PSI-LHCI supercomplex is its extremely high efficiency of energy transfer, and it is estimated that the energy absorbed by LHCI may induce charge separation with an efficiency close to 100% [1].

The structure of cyanobacterial PSI core trimer has been solved at a resolution of 2.5 Å, revealing the detailed organization and arrangements of subunits and various pigments [2]. The structure of plant PSI-LHCI was solved first at 4.4 Å resolution by the Nelson group, and the resolution limits were gradually improved to 3.3 Å [3,4,5]. These structures showed that the architecture of the PSI core is largely unchanged from cyanobacterial PSI core [2] over 3 billion years of evolution, and that each of the Lhca1-Lhca4 subunits shares a general folding and some common binding sites for chlorophylls (Chls) as seen in the LHC protein family [6-9]. However, due to the limited resolution the exact position and number of cofactors associated with each of the LHCI subunits were not resolved, which have hampered the understanding of the mechanisms of light capturing, excitation energy transfer and dissipation within the PSI-LHCI supercomplex. Recently, we succeeded in solving the structure of PSI-LHCI from pea at 2.8 Å resolution [10••], which was followed by another report by Nelson's group at the same resolution [11••]. Although there are some slight differences between the two structures in relation to the species, position and numbers of cofactors associated with LHCI, these structures revealed the detailed organization of protein subunits and various cofactors. In this review, we summarize the overall structure briefly, and then focus on the excitation energy transfer pathways and photoprotection mechanisms based on the structure obtained. Other mechanisms related to the PSI-LHCI structure can be found in [12-16].

Overall structure

The PSI-LHCI supercomplex is composed of two functional moieties: the PSI core and the peripheral LHCI. The PSI core contains nine membrane-embedded PsaA, PsaB, PsaF, PsaG, PsaH, PsaI, PsaJ, PsaK, PsaL, and three hydrophilic, peripheral subunits PsaC, PsaD and PsaE. Among these subunits, the PsaG and PsaH membrane-spanning subunits are unique to plant and not found in cyanobacterial PSI [2]. LHCI contains four trans-membrane Lhca proteins arranged as a dimer of hetero dimers between Lhca1/Lhca4 and Lhca2/Lhca3, and forms a belt associated with the PsaF side of the PSI core (Figure 1a-b). Intensive interactions are formed between Lhca1 and the PSI core subunits PsaB, PsaG, and between Lhca3 and PsaA, PsaK, at both stromal and lumenal sides, while interactions between Lhca2 and the PSI core subunit PsaJ and between Lhca4 and PsaF are rather weak and limited to the stromal side. This results in a hollow between the PSI core and LHCI at the lumenal side, which may allow regulatory co-factors and proteins to come in to interact with LHCI and the PSI core during light-energy dissipation. In addition to the protein subunits, a total of 205 cofactors were identified in the PSI-LHCI supercomplex [10••]. These include 155 Chls (143 Chls *a* and 12 Chls *b*), 35 carotenoids [26 β-carotenes (BCRs), five luteins (Luts), and four violaxanthins (Vios)], three Fe_4S_4 clusters, two phylloquinones (Figure 1). Among them, the PSI core contains 98 Chls *a*, 22 BCRs, three Fe_4S_4 clusters and two phylloquinones, whereas LHCI contains 45 Chls *a*, 12 Chls *b*, four BCRs, five Luts and four Vios.

Comparison of the pigments between the plant and cyanobacterial PSI core reveals how their positions and orientations are maintained, adjusted or newly achieved during the evolutionary process. Out of the 96 Chls and 22 BCRs reported in the cyanobacterial PSI structure [2], two Chls and two BCRs are missing in the higher plant PSI core. Among the remaining 94 Chls and 20 BCRs, eleven Chls and eight BCRs slightly changed their positions and orientations, while 83 Chls and 12 BCRs remained unchanged. Furthermore, four Chls and two BCRs bound to new sites in the plant PSI core (Figure 1c-e). All these changes are found to be located at the "peripheral" rather than the "core" region of the PSI core, and can be categorized into two groups: (i) on the PsaH side (cyanobacterial PSI monomer-monomer interface side), and (ii) on the LHCI

side. In the former case, the changes are likely due to the loss of PsaM and/or the addition of PsaH in the higher plant PSI, and some of the changes are located close to the putative binding site for the main light-harvesting-complex II (LHCII) based on single particle analysis [17]. These changes may facilitate energy transfer from LHCII to the PSI core upon formation of a PSI-LHCI-LHCII super-supercomplex under the "state II" condition [18]. In fact, time-resolved fluorescence measurements of PSI-LHCI-LHCII super-supercomplex of *Chlamydomonas reinhardtii* showed that Chl *a*1401 in PsaK, a Chl whose position was shifted significantly in plant PSI, could be involved in energy transfer pathways from Chl *a*605 of LHCII to the PSI core [19]. On the LHCI side, the changes may be caused by the loss of PsaX and/or addition of PsaG and LHCI in plant PSI, which may maximize the efficiency of energy transfer from LHCI to the PSI core as described below.

In spite of the slight changes described above, most of the Chls and BCRs remained largely unchanged from cyanobacterial to the plant PSI core, suggesting that the excitation energy transfer kinetics and pathways may be largely similar between them. However, cyanobacterial PSI core contains "red Chls", whereas most of the red Chls are located in LHCI in the higher plant PSI-LHCI supercomplex (see below). Thus, some differences are expected in the energy migration mechanism between the cyanobacterial and plant PSI core.

Energy transfer pathways from LHCI to PSI core

The excitation energy transfer (EET) efficiency is close to 100% in the plant PSI-LHCI supercomplex, which means that almost all of the photons absorbed by LHCI may be utilized to initiate the charge separation at the PSI reaction center [1,16]. A number of studies have been carried out to elucidate the pathways and mechanism for this highly efficient EET process in the PSI-LHCI complex [20-28]. These studies showed that the light-induced charge separation at P700, the reaction center of PSI, occurs very fast with a lifetime of ~6 ps, whereas the energy-trapping at the reaction center is rather slow with a trapping lifetime of 50 ps, indicating that the whole EET process is trap-limited. Furthermore, several pair of red Chls that absorbs lower energy than the PSI reaction center due to a strong coupling between two Chl molecules, were found to be present in

Lhca subunits and play important roles in the EET.

Structural analysis of the PSI-LHCI supercomplex yielded important information regarding the EET pathways and mechanism within the supercomplex. It was revealed that each of the four Lhca subunits has a pair of red Chls (Chl 603-609) located in the stromal side interface between Lhca and the PSI core, connecting LHCI with the PSI core. This well explains why a large part of the EET goes through the red Chls [14]. The phytol tails of these red Chls protrude into "the gap region" between LHCI and the PSI core, which may not only anchor the Lhca subunits to the PSI core, but is also suited to collecting the excited energy from neighboring pigments and transferring it to the PSI core.

In spite of the common general features of the protein and pigment arrangement of the Lhcas, there are apparent differences in interactions between each of the Lhca subunits and the PSI core, leading to possible differences in the EET efficiency from the individual Lhca subunit to the PSI core. Lhca1 and Lhca3 in the two sides of the LHCI belt were found to have stronger interactions with the PSI core, whereas Lhca2 in the middle of the belt interacts with the PSI core rather weakly, and Lhca4 has almost no direct interaction with the core. Based on the strengths of interactions between Lhcas and the PSI core, the following EET pathways were identified: 1Bl/1Bs, 1Fl, 2Jl, and 3Al/3As (which are named in the order of the number of Lhca subunit-PSI core subunit-stromal or lumenal side interaction) (Table 1, Figure2) [10••]. The 1Bl pathway has a connection between *b*607 of Lhca1 with three Chls (*a*1231, *a*1232 and *a*1233) of the PsaB subunit at the lumenal side, with a shortest edge-to-edge distance of 5.5 Å. Importantly, the three Chls (*a*1231, *a*1232, and *a*1233) are proposed as the putative red Chls in the cyanobacterial PSI core [2], and Chl *a*1233 in the plant PSI core changed its ring position significantly compared to the cyanobacterial one, resulting in an ideal short distance from Chl *b*607 of Lhca1. However, since energy transfer from Chl *a* to Chl *b* is inefficient in general, Chl *b*607 may partially limit the energy transfer, or the binding site may be able to bind both Chl *a* and Chl *b* as seen in LHCII and a minor LHCII component CP29 [8,29-33]. The 1Bs pathway transfers the energy from the red Chl pair *a*603-*a*609 of Lhca1 to three Chls (*a*1218, *a*1219, and *a*1802) of PsaB at the

stromal side (Figure 2b-c), with a shortest edge-to-edge distance of 7.5 Å (Table 1), suggesting that this pathway is highly efficient. The Chl *a*1802 is one of the newly achieved Chls in the plant PSI core during the evolution from cyanobacteria to plants, which is accompanied by significant structural changes in a loop region connecting transmembrane helices *d* and *e* of PsaB. The middle part of the loop region (Ala^{307}-Gly^{318}) of PsaB flipped by about 10 Å toward the PSI core with a flipping angle of about 60 degree. A Chl *a*40 in the similar position to Chl *a*1802 of the plant PSI core was found in the structure of a monomeric *Synechocystis* PSI core, and Mazor et al. suggested that the Chl trimer (*a*1218, *a*1219, and *a*40) may be the red Chls [34].

The 1Fl pathway transfers energy from Chl *a*616 of Lhca1 to Chl *a*1701 of the PsaF subunit in the lumenal side, with a shortest edge-to-edge distance of 8.2 Å (Table 1). The chlorine ring of Chl *a*1701 has a significant positional shift of 9 Å in comparison with the cyanobacterial PSI, which may facilitate the EET through this pathway. The Chls in Lhca4 have no direct interactions with those of the core, and its Chls are rather closer to Lhca1. In particular, an edge-to-edge distance of 5.9 Å was found between *a*616 of Lhca1 and *a*617 of Lhca4. Thus, the energy absorbed by Lhca4 may be transferred to the PSI core through the 1Fl pathway (Figure 2d). In the stromal side, the 1Bs pathway may also accept energy from Lhca4 and transfer them to the core.

In the 2Jl pathway, the shortest edge-to-edge distance is 12.8 Å between Chl *b*607 of Lhca2 and *a*1302 of PsaJ in the lumenal side. Due to the presence of a Chl *b* and the rather long distance, it seems that the energy transfer from Lhca2 to the PSI core is not very efficient. This is different from the fast EET kinetics estimated from picosecond fluorescence spectroscopic studies [28]. However, weak electron densities were observed in “the gap region” between Lcha2 and the PSI core in our structure analysis which were not assigned in the model; these densities may represent an additional Chl [10••]. Alternatively, the gap region may undergo dynamic structural changes under physiological conditions to facilitate the energy transfer.

The shortest edge-to-edge distances between pigments of Lhca3 and PsaA are 5.8 Å and 10.2 Å in the lumenal and stromal side, respectively, forming the 3Al and 3As pathways

(Figure 2f-g, Table 1). The 3Al pathway may transfer energy through both the red Chl pair *a*603-*a*609 and other Chls, whereas the 3As pathway collects energy mostly through the red Chl pair. There are also Chls of Lhca2 that are close to these pathways, suggesting that the energy absorbed by Lhca2 may also be transferred to the core through these pathways in Lhca3.

It should be mentioned that both structures from the two groups [10••,11••] contained much less Chls in the gap region than the previous structures determined at lower resolutions [3,4,5]. Because many previous studies have been performed on the basis of the structure containing those gap Chls, re-examinations of those results may be necessary based on the new structures. To summarize, the red forms play important roles in EET from LHCI to the core, whereas other pathways are also present that do not involve the red Chls. However, there may be some ambiguities in the position and orientation of some of the pigments in the current structure due to the limited resolution, and further refined structures are required to reveal the full picture of EET in this enormously large pigment-protein complex.

Photoprotection and nonphotochemical quenching mechanisms

Our structural analysis identified a total of 13 carotenoids in the four Lhca subunits, with each Lhca binding three carotenoids (one Lut, one Vio, and one BCR) at three sites (L1, L2, and N1, respectively) and an additional lutein (Lut624) bound in the interface between Lhca1 and Lhca4 (Figure 3). This is in comparison with 10 carotenoids (9 Luts and 1 BCR) reported by Mazor et al. [11••]. Importantly, we found that each Lhca subunit binds one Vio at its "L2" site. Vio is known to be converted to zeaxanthin (Zea) by de-epoxidation via Vio deepoxidase (VDE) upon acidification in the lumen induced by excess light illumination, thereby triggering the xanthophyll cycle. This is a cycle of interconversion between Vio and Zea. Upon conversion of Vio into Zea, the light energy is dissipated through the Zea-binding site; thus, the xanthophyll cycle is important for energy dissipation under excess light illumination, a process known as Zea-dependent non-photochemical quenching (NPQ) [35,36]. This process is important for photoprotection under strong light illumination.

The xanthophyll cycle has been found and studied in LHCII extensively [37,38]. Recently, the Zea-dependent NPQ in LHCI has also been reported [39•], and our structure provided evidence for the possible operation of this mechanism in LHCI. In the crystal structure, the Vio is located in a groove formed by two transmembrane helices A and B of Lhca subunits that face the PSI core. When VDE binds to the lumenal side to catalyze de-epoxidation, the two Lhca subunits (Lhca2 and Lhca4) in the middle of the LHCI belt would be more accessible than the side ones (Lhca1 and Lhca3) because of the deep “hollow” in the middle between LHCI and the PSI core. In addition, the lumenal end of the Vio in each Lhca is surrounded by three Chls (*a*604, *a*/*b*606, *a*/*b*607) and capped by the loop between transmembrane helices A and C (AC loop), and differences are also found in the organization of the AC loops between Lhca2/4 and Lhca1/3. The AC loops of Lhca2 and Lhca4 consist of 21 residues and bind Chl *b*607 indirectly via water molecules, whereas the AC loops of Lhca3 and Lhca1 are ten residues longer in order to make interactions with the PSI core, and coordinate Chl *a*/*b*607 directly. These structural differences imply that the AC loops of Lhca2 and Lhca4 are more flexible and may allow larger dynamic structural changes to occur than that of Lhca1 and Lhca3, making the Vio in Lhca2/4 more likely to be involved in the xanthophyll cycle. Furthermore, differences are also found in the hydrogen-bonding pattern between the Vio bound to Lhca1/3 and that bound to Lhca2/4. In Lhca2 and Lhca4, only one hydrogen-bond is found between the hydroxyl group of Vio (pointing to the lumenal side) and a carbonyl oxygen atom from the main chain of Trp 127^{Lhca2} and Trp 126^{Lhca4}, whereas the Vio bound to Lhca1 and Lhca3 makes one additional hydrogen-bond (to Gln 105^{Lhca1} and Thr 133^{Lhca3} respectively). This suggests that the affinity for Vio is lower in the middle Lhcas than that in the two side Lhca subunits (Lhca1/3). Based on these structural features, we propose that Zea-dependent NPQ may function more efficiently in the middle Lhcas than that in the side Lhcas.

Conclusions

The structural analysis of the plant PSI-LHCI supercomplex at a resolution of 2.8 Å reveals many new features of the arrangement of protein subunits and cofactors of this extremely large membrane-protein complex, such as the first identification of Chl *b* from Chl *a*, clarification of many Chls assigned in the "gap region" between LHCI and

the PSI core in the previous low-resolution structures, and identification of the Vio-binding sites in each of the Lhca subunits. These results provide a basis for elucidating the mechanism of highly efficient energy transfer from LHCI to the PSI core, and possible photoprotection mechanism under excess light illumination. On the other hand, there is still a need for higher-resolution structures in order to fully reveal the mechanisms of energy transfer, electron transfer, and photoprotection occurring within this supercomplex. Given the recent developments in high-resolution structural analysis of large membrane-protein complexes such as photosystem II [40, 41], advancement on the structural analysis of the PSI-LHCI complex may be expected in the near future.

Acknowledgements

We apologize to all the researchers whose papers could not be cited in this review because of the limited space. The authors acknowledge the program for promoting the enhancement of research universities at Okayama University, JSPS KAKENHI Grant Nos. 24000018 (J.-R.S.) and 26840023 and 15H01642 (M.S.) from MEXT, Japan, National Basic Research Program of China (Nos. 2011CBA00901, 2015CB150101), and Youth Innovation Promotion Association of CAS, China for financial support.

Reference and recommended reading

Papers of particular interest, published within the period of review have been highlighted as:

• of special interest

• • of outstanding interest

1. Nelson N: **Plant Photosystem I - The Most Efficient Nano-Photochemical Machine**. *Journal of Nanoscience And Nanotechnology* 2009, **9**:1709-1713.

2. Jordan P, Fromme P, Witt HT, Klukas O, Saenger W, Krauss N: **Three-dimensional structure of cyanobacterial photosystem I at 2.5 A resolution**. *Nature* 2001, **411**:909-917.

3. Ben-Shem A, Frolow F, Nelson N: **Crystal structure of plant photosystem I**. *Nature* 2003, **426**:630-635.

4. Amunts A, Drory O, Nelson N: **The structure of a plant photosystem I supercomplex at 3.4 A resolution**. *Nature* 2007, **447**:58-63.

5. Amunts A, Toporik H, Borovikova A, Nelson N: **Structure determination and improved model of plant photosystem I**. *J Biol Chem* 2010, **285**:3478-3486.

6. Liu Z, Yan H, Wang K, Kuang T, Zhang J, Gui L, An X, Chang W: **Crystal structure of spinach major light-harvesting complex at 2.72 A resolution**. *Nature* 2004, **428**:287-292.

7. Standfuss J, Terwisscha van Scheltinga AC, Lamborghini M, Kuhlbrandt W: **Mechanisms of photoprotection and nonphotochemical quenching in pea light-harvesting complex at 2.5 A resolution**. *EMBO J* 2005, **24**:919-928.

8. Pan X, Li M, Wan T, Wang L, Jia C, Hou Z, Zhao X, Zhang J, Chang W: **Structural insights into energy regulation of light-harvesting complex CP29 from spinach**. *Nat Struct Mol Biol* 2011, **18**:309-315.

9. Pan XW, Liu ZF, Li M, Chang WR: **Architecture and function of plant light-harvesting complexes II**. *Current Opinion in Structural Biology* 2013, **23**:515-525.

10. Qin X, Suga M, Kuang T, Shen JR: **Structural basis for energy transfer pathways in the plant PSI-LHCI supercomplex**. *Science* 2015, **348**:989-995.

• • The first high-resolution structure of plant PSI-LHCI supercomplex solved at 2.8 Å resolution., showing the precise positions and orientaions of most of the co-factors in the PSI-LHCI supercomplex. The possible EET pathways are proposed based on the structure.

11. Mazor Y, Borovikova A, Nelson N: **The structure of plant photosystem I super-complex at 2.8 Å resolution**. *elife* 2015, **4**:e07433.

• • The structure of the plant PSI-LHCI supercomplex reported a few months later than ref. [10] at the same resolution. Slight differences in the organization of the pigments and other cofacters can be found between the two structures, especially with respect to those of LHCI.

12. Melkozernov AN, Blankenship RE: **Structural and functional organization of the peripheral light-harvesting system in photosystem I**. *Photosynth Res* 2005, **85**:33-50.

13. Croce R, van Amerongen H: **Light-harvesting and structural organization of Photosystem II: from individual complexes to thylakoid membrane**. *J Photochem Photobiol B* 2011, **104**:142-153.

14. Croce R, van Amerongen H: **Light-harvesting in photosystem I**. *Photosynth Res* 2013,

116:153-166.
15. Croce R, van Amerongen H: **Natural strategies for photosynthetic light harvesting**. *Nat Chem Biol* 2014, **10**:492-501.
16. Nelson N, Junge W: **Structure and Energy Transfer in Photosystems of Oxygenic Photosynthesis**. *Annu Rev Biochem* 2015.
17. Kouril R, Zygadlo A, Arteni AA, de Wit CD, Dekker JP, Jensen PE, Scheller HV, Boekema EJ: **Structural characterization of a complex of photosystem I and light-harvesting complex II of Arabidopsis thaliana**. *Biochemistry* 2005, **44**:10935-10940.
18. Kyle DJ, Staehelin LA, Arntzen CJ: **Lateral mobility of the light-harvesting complex in chloroplast membranes controls excitation energy distribution in higher plants**. *Arch Biochem Biophys* 1983, **222**:527-541.
19. Le Quiniou C, van Oort B, Drop B, van Stokkum IH, Croce R: **The High Efficiency of Photosystem I in the Green Alga Chlamydomonas reinhardtii Is Maintained after the Antenna Size Is Substantially Increased by the Association of Light-harvesting Complexes II**. *J Biol Chem* 2015, **290**:30587-30595.
20. Gobets B, van Grondelle R: **Energy transfer and trapping in photosystem I**. *Biochimica Et Biophysica Acta-Bioenergetics* 2001, **1507**:80-99.
21. Ihalainen JA, Jensen PE, Haldrup A, van Stokkum IH, van Grondelle R, Scheller HV, Dekker JP: **Pigment organization and energy transfer dynamics in isolated photosystem I (PSI) complexes from *Arabidopsis thaliana* depleted of the PSI-G, PSI-K, PSI-L, or PSI-N subunit**. *Biophys J* 2002, **83**:2190-2201.
22. Ihalainen JA, Ratsep M, Jensen PE, Scheller HV, Croce R, Bassi R, Korppi-Tommola JEI, Freiberg A: **Red spectral forms of chlorophylls in green plant PSI - a site-selective and high-pressure spectroscopy study**. *Journal of Physical Chemistry B* 2003, **107**:9086-9093.
23. Morosinotto T, Breton J, Bassi R, Croce R: **The nature of a chlorophyll ligand in Lhca proteins determines the far red fluorescence emission typical of photosystem I**. *J Biol Chem* 2003, **278**:49223-49229.
24. Croce R, Morosinotto T, Ihalainen JA, Chojnicka A, Breton J, Dekker JP, van Grondelle R, Bassi R: **Origin of the 701-nm fluorescence emission of the Lhca2 subunit of higher plant photosystem I**. *J Biol Chem* 2004, **279**:48543-48549.
25. Engelmann E, Zucchelli G, Casazza AP, Brogioli D, Garlaschi FM, Jennings RC: **Influence of the photosystem I-light harvesting complex I antenna domains on fluorescence decay**. *Biochemistry* 2006, **45**:6947-6955.
26. Slavov C, Ballottari M, Morosinotto T, Bassi R, Holzwarth AR: **Trap-limited charge separation kinetics in higher plant photosystem I complexes**. *Biophys J* 2008, **94**:3601-3612.
27. Wientjes E, Oostergetel GT, Jansson S, Boekema EJ, Croce R: **The Role of Lhca complexes in the supramolecular organization of higher plant photosystem I**. *Journal of Biological Chemistry* 2009, **284**:7803-7810.
28. Wientjes E, van Stokkum IH, van Amerongen H, Croce R: **The role of the individual Lhcas in photosystem I excitation energy trapping**. *Biophys J* 2011, **101**:745-754.

29. Rogl H, Kuhlbrandt W: **Mutant trimers of light-harvesting complex II exhibit altered pigment content and spectroscopic features**. *Biochemistry* 1999, **38**:16214-16222.
30. Remelli R, Varotto C, Sandona D, Croce R, Bassi R: **Chlorophyll binding to monomeric light-harvesting complex. A mutation analysis of chromophore-binding residues**. *J Biol Chem* 1999, **274**:33510-33521.
31. Rogl H, Schodel R, Lokstein H, Kuhlbrandt W, Schubert A: **Assignment of spectral substructures to pigment-binding sites in higher plant light-harvesting complex LHC-II**. *Biochemistry* 2002, **41**:2281-2287.
32. Yang C, Kosemund K, Cornet C, Paulsen H: **Exchange of pigment-binding amino acids in light-harvesting chlorophyll a/b protein**. *Biochemistry* 1999, **38**:16205-16213.
33. Bassi R, Croce R, Cugini D, Sandona D: **Mutational analysis of a higher plant antenna protein provides identification of chromophores bound into multiple sites**. *Proc Natl Acad Sci U S A* 1999, **96**:10056-10061.
34. Mazor Y, Nataf D, Toporik H, Nelson N: **Crystal structures of virus-like photosystem I complexes from the mesophilic cyanobacterium Synechocystis PCC 6803**. *elife* 2014, **3**:e01496.
35. Arnoux P, Morosinotto T, Saga G, Bassi R, Pignol D: **A structural basis for the pH-dependent xanthophyll cycle in Arabidopsis thaliana**. *Plant Cell* 2009, **21**:2036-2044.
36. Pfundel E, Bilger W: **Regulation and possible function of the violaxanthin cycle**. *Photosynth Res* 1994, **42**:89-109.
37. Jahns P, Wehner A, Paulsen H, Hobe S: **De-epoxidation of violaxanthin after reconstitution into different carotenoid binding sites of light-harvesting complex II**. *J Biol Chem* 2001, **276**:22154-22159.
38. Jahns P, Latowski D, Strzalka K: **Mechanism and regulation of the violaxanthin cycle: the role of antenna proteins and membrane lipids**. *Biochim Biophys Acta* 2009, **1787**:3-14.
39. Ballottari M, Alcocer MJ, D'Andrea C, Viola D, Ahn TK, Petrozza A, Polli D, Fleming GR, Cerullo G, Bassi R: **Regulation of photosystem I light harvesting by zeaxanthin**. *Proc Natl Acad Sci U S A* 2014, **111**:E2431-2438.
• The first report of zeaxanthin-dependent energy dissipation in PSI based on fluorescence measurements of PSI-LHCI complexes from a non-photochemical quenching mutant.
40. Umena Y, Kawakami K, **Shen JR**, Kamiya N: **Crystal structure of oxygen-evolving photosystem II at a resolution of 1.9 Å.** *Nature* 2011, **473**:55-60.
41. Suga M, Akita F, Hirata K, Ueno G, Murakami H, Nakajima Y, Shimizu T, Yamashita K, Yamamoto M, Ago H, Shen JR: **Native structure of photosystem II at 1.95 Å resolution viewed by femtosecond X-ray pulses.** *Nature* 2015, **517**:99-103.

Figure legends

Figure 1 Structure of the plant PSI-LHCI supercomplex and its comparison with cyanobacterial PSI. Stereo views of the overall structure of the supercomplex with a view from the LHCI side (**a**) and a view along the membrane normal from the stromal side (**b**). **c**, The arrangement of cofactors with the view direction same as in panel **b**. Color code: red, Chls involved in the electron transfer chain (ETC) and red Chls; magenta, Chls and BCRs that are newly found or having significant positional shift in the plant PSI core; green, other Chls in the PSI core; gray, Chls and carotenoids in LHCI. Numbers indicate Chls of the PSI core involved in the EET pathways. **d**, The arrangement of cofactors of cyanobacterial PSI with the view direction same as in panel **b**. Color code: cyan, Chls and BCRs that were not found in the plant PSI core; brown, Chls and BCRs that have slight positional movements between plant and cyanobacterial PSI; black, Chls involved in ETC, and the other Chls and BCRs which are found to be in equivalent positions and orientations between the plant and cyanobacterial PSI core. Overlay of panels **c** and **d**.

Figure 2 Possible EET pathways from LHCI to the PSI core. a, Overall location of pigments involved in EET pathways from LHCI to the PSI core. Locations of the Red Chls in each Lhca subunits and the putative binding site of LHCII are represented by red ovals and a blue circle, respectively. Spheres indicate magnesium ions of Chls. Arrows in panels (**a-g)** indicate the possible EET pathways from LHCI to the PSI core. Red color and blue color of the arrows indicate the pathways either in the liminal side or the stromal side, respectively. **b**, Stromal side EET pathway 1Bs from Lhca1 to PsaB in the PSI core. **c**, Stromal and lumenal EET pathways 1Bs and 1Bl from Lhca1 to PsaB in the PSI core. In panels (**b**, **c**), plant and cyanobacterial loop regions connecting the transmembrane helices *d* and *e* in PsaB are colored in red and magenta, respectively. **d**, Lumenal side EET pathway 1Fl from Lhca1 to PsaF in the PSI core. **e**, Lumenal side EET pathway 2Jl from Lhca2 to PsaJ in the PSI core. **f** and **g**, Stromal and lumenal EET pathways 3As and 3Al from Lhca3 to PsaA in the PSI core. Color code for cofactors for panels **b**-**g**: red, red Chls; magenta, Chls newly found in plant PSI or having significant positional change from cyanobacterial PSI; orange, Chls and BCRs having slight positional change from cyanobacterial PSI; green, Chls remain unchanged between cyanobacterial and plant PSI; blue, BCRs remain unchanged between cyanobacterial

and plant PSI; gray, Chls and carotenoids in LHCI; black, Chls and BCRs in cyanobacterial PSI. The phytol chains of Chls except red Chls were omitted for clarity. View directions are from the stromal side for panels **a**, **b**, **d**, **e** and **f**, and perpendicular to the membrane normal for panels **c** and **g**.

Figure 3 Arrangement of carotenoids in LHCI. a, Top view along the membrane normal from the stromal side. **b**, Side view of LHCI. The three carotenoid binding sites L1 (Lut 620), L2 (Vio 621) and N1 (BCR 623) in each Lhca subunit were shown in green, yellow and magenta, respectively. Lut 624 in the L3 site of Lhca4 was shown in light blue. Chls *a* and *b* were shown in gray and orange, respectively.

463 **Table 1. Major energy transfer pathways from Lhcas to PSI core.**

Pathways	Lumenal or Stromal	Lhca	Chl (Lhca)		PSI core	Chl (PSI core)		Distance (Å)[1]	Red Chls[2]	Remarks[3]
			PDB #	LHCII #		PDB #	LHCII #			
1Bl	L	a1	307	*b*607	B	**101(G)**	***a*1233**	5.5	N	–
1Bs	S	a1	304, 309	*a*603, *a*609	B	821, **822, 841**	*a*1218, ***a*1219, *a*1802**	7.5	Y	Lhca4
1Fl	L	a1	315	*a*616	F	**304**	***a*1701**	8.2	N	Lhca4 (Red Chl)
2Jl	L	a2	606	*b*607	J	**3002**	***a*1302**	12.8	Y/N	–
3Al	L	a3	306	*a*607	A	**817**	***a*1114**	5.8	N	Lhca2
3As	S	a3	303, 308, 315	*a*603, *a*609, *a*619	A	**811,** 813	***a*1108,** *a*1110	10.2	Y	Lhca2

464 Bold characters indicate structures significantly changed compared with those in
465 cyanobacterial PSI core.
466 [1]Shortest edge-to-edge distances.
467 [2]Involving the red Chls or not.
468 [3]Energy from other Lhcas (red Chls indicating involvement of the red Chls) may also be
469 transferred through this pathway.
470

Figure

Click here to download high resolution image

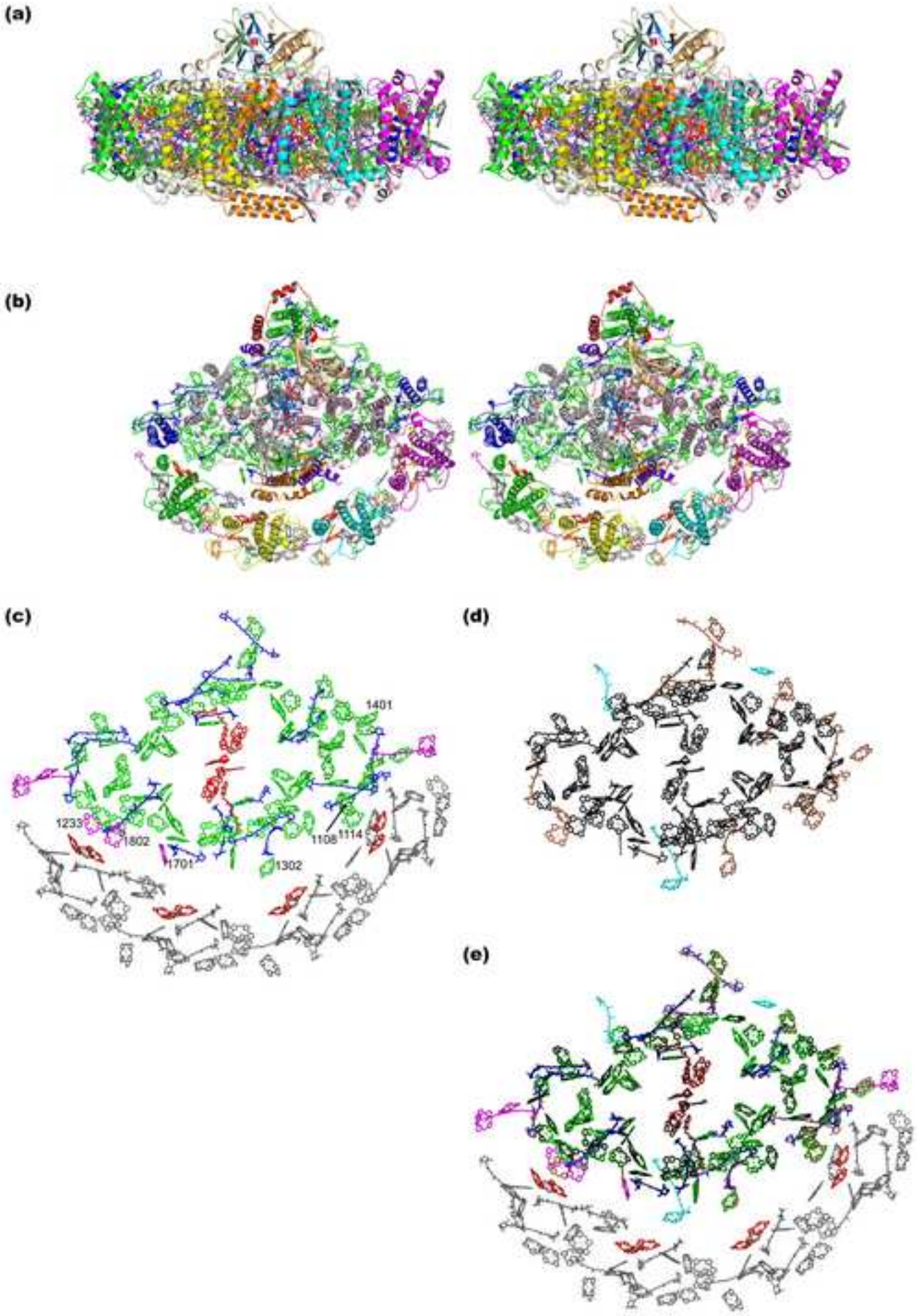

Figure

Click here to download high resolution image

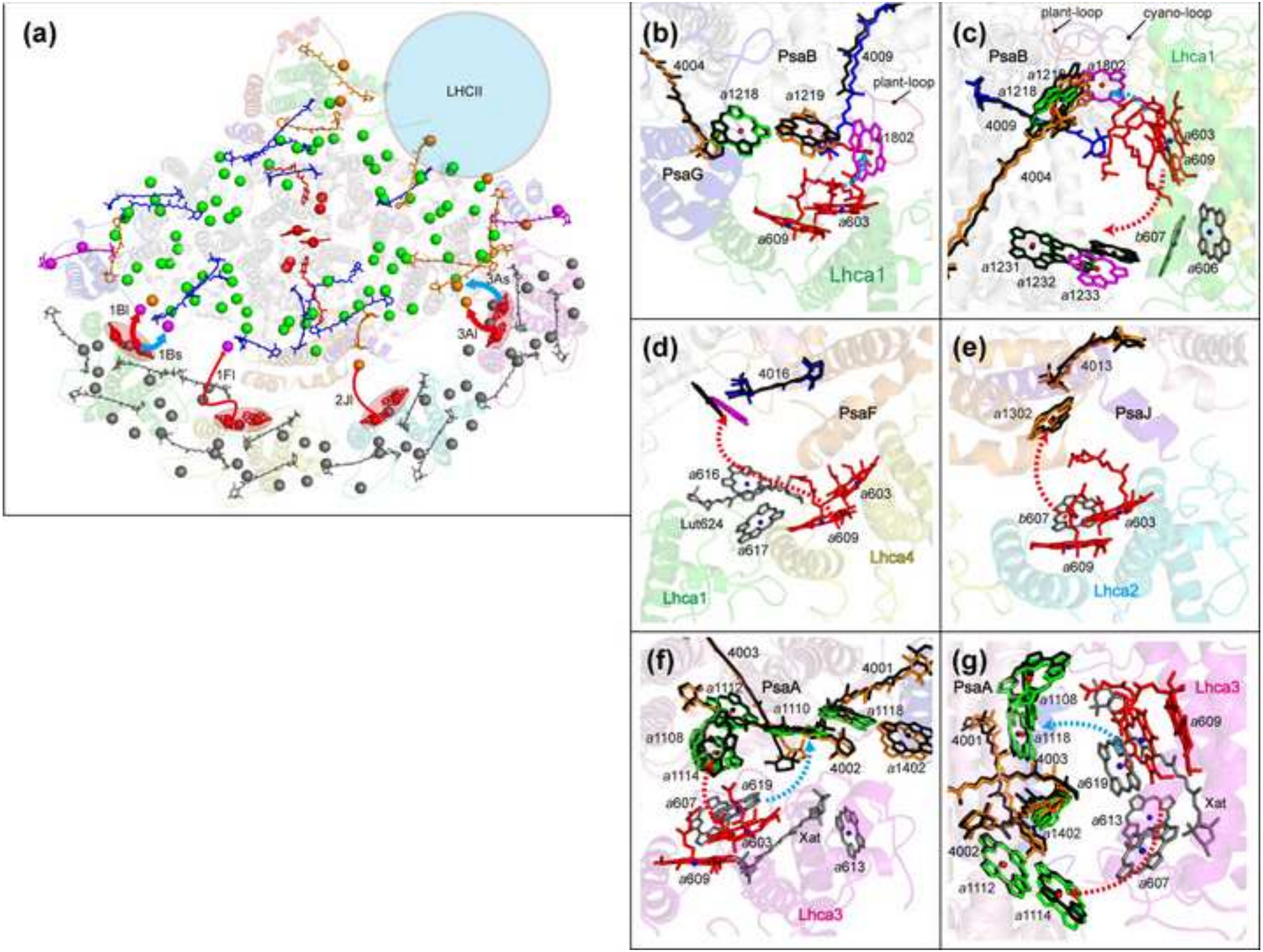

Figure
Click here to download high resolution image